JOURNAL OF PETROLOGY | VOLUME 45 | NUMBER 11 | PAGES 2155–2170 | 2004 | doi:10.1093/petrology/egh051

Residence, Resorption and Recycling of Zircons in Devils Kitchen Rhyolite, Coso Volcanic Field, California

JONATHAN S. MILLER[1]* AND JOSEPH L. WOODEN[2]

[1]DEPARTMENT OF GEOLOGY, SAN JOSE STATE UNIVERSITY, ONE WASHINGTON SQUARE, SAN JOSE, CA 95192-0102, USA

[2]US GEOLOGICAL SURVEY, STANFORD–USGS MICRO-ANALYTICAL CENTER, SCHOOL OF EARTH SCIENCES, STANFORD UNIVERSITY, GREEN EARTH SCIENCES BUILDING, STANFORD, CA 94305-2220, USA

RECEIVED DECEMBER 3, 2002; ACCEPTED JUNE 26, 2004
ADVANCE ACCESS PUBLICATION AUGUST 27, 2004

Zircons from the Devils Kitchen rhyolite in the Pleistocene Coso Volcanic field, California have been analyzed by in situ *Pb/U ion microprobe (SHRIMP-RG) and by detailed cathodoluminescence imaging. The zircons yield common-Pb-corrected and disequilibrium-corrected $^{206}Pb/^{238}U$ ages that predate a previously reported K–Ar sanidine age by up to 200 kyr, and the range of ages exhibited by the zircons is also approximately 200 kyr. Cathodoluminescence imaging indicates that zircons formed in contrasting environments. Most zircons are euhedral, and a majority of the zircons are weakly zoned, but many also have anhedral, embayed cores, with euhedral overgrowths and multiple internal surfaces that are truncated by later crystal zones. Concentrations of U and Th vary by two orders of magnitude within the zircon population, and by 10–20 times between zones within some zircon crystals, indicating that zircons were transferred between contrasting chemical environments. A zircon saturation temperature of ~750°C overlaps within error a previously reported phenocryst equilibration temperature of 740 ± 25°C. Textures in zircons indicative of repeated dissolution and subsequent regrowth are probably caused by punctuated heating by mafic magma input into rhyolite. The overall span of ages and large variation in U and Th concentrations, combined with calculated zircon saturation temperatures and resorption times, are most compatible with crystallization in magma bodies that were emplaced piecemeal in the crust at Coso over 200 kyr prior to eruption, and that were periodically rejuvenated or melted by subsequent basaltic injections.*

KEY WORDS: *zircon geochronology; residence time; rhyolite; ion microprobe; California*

INTRODUCTION

Evaluating the dynamic evolution of silicic magma systems depends critically on knowing the time-scales over which magma generation, ascent, emplacement, storage, recharge, solidification and eruption occur. For shallow, crystal-poor, silicic magma bodies (i.e. sub-volcanic systems), knowledge of magma residence time is vital to a full explanation of their long-term dynamic evolution and eruptive behavior. A variety of approaches (theoretical, experimental, geochemical and geochronometric) have been used in recent years to address time-scales and rates of magmatic processes in igneous systems (see summaries in Hawkesworth *et al.*, 2000, 2004). However, the longevity of silicic magma bodies in the crust, their physical state changes through time and their physical and chemical responses to long-term vs transient inputs and outputs of mass and heat (e.g. Spera & Bhorson, 2001; Bachmann *et al.*, 2002) remains far from complete.

In this work, we utilize *in situ* ion probe analysis of zircon, combined with cathodoluminescence (CL) imaging to examine the growth history of zircons from a single rhyolite dome from the Coso Volcanic field, California: a Pleistocene silicic magma system. We then use these results to discuss the evolution of the magma system that fed the dome. In contrast to many of the previous zircon studies of young rhyolite systems, the Coso Volcanic field appears to be growing, and is, arguably, still in its infancy (Bacon, 1982). The zircons that we have examined in this study are from the earliest

*Corresponding author. E-mail: jsmiller@email.sjsu.edu

rhyolite dome eruption. As such, they reveal the organization and assembly of a rhyolite system at its most juvenile stage.

Use of magmatic zircons to examine magma residence and storage exploits either radioactive decay of $^{238}U \rightarrow ^{230}Th$ or $^{238}U \rightarrow ^{206}Pb$ in the zircons (e.g. Reid *et al.*, 1997; Brown & Fletcher, 1999; Bacon *et al.*, 2000; Lowenstern *et al.*, 2000; Reid & Coath, 2000; Bindeman *et al.*, 2001; Sano *et al.*, 2002; Vazquez & Reid, 2002; Schmitt *et al.*, 2003). U–Th disequilibria studies are suitable for magmatic systems with ages of less than approximately 350 ka (approximately 5 half-lives for $^{238}U \rightarrow ^{230}Th$), after which secular equilibrium obtains. In this study, we use the $^{238}U \rightarrow ^{206}Pb$ method.

Zircons offer some distinct advantages, compared with other methods of investigating crystal (and magma) residence and magma history, because they commonly begin crystallizing early in felsic magmas (once appropriate levels of Zr concentration are achieved). Thus, given sufficient time and analytical precision, it is possible to resolve multiple pulses of magma input and zircon crystal growth. Also, the crystallization and dissolution behavior of zircon in magmas and their Pb, Th, and U diffusion properties are well known (e.g. Harrison & Watson, 1983; Watson & Harrison, 1983; Watson, 1996; Cherniak *et al.*, 1997; Lee *et al.*, 1997; Hoskin *et al.*, 2000). Thus, they are not merely chronometers, but are also sensitive indicators of fluctuating chemical and thermal conditions in magma bodies (see Robinson & Miller, 1999; Hoskin *et al.*, 2000). The well-established diffusion parameters for zircon also allow crystal dissolution and growth times to be estimated (Watson, 1996), which potentially provides further information on period(s) of solidification and magmatic residence time of zircons in silicic magma bodies.

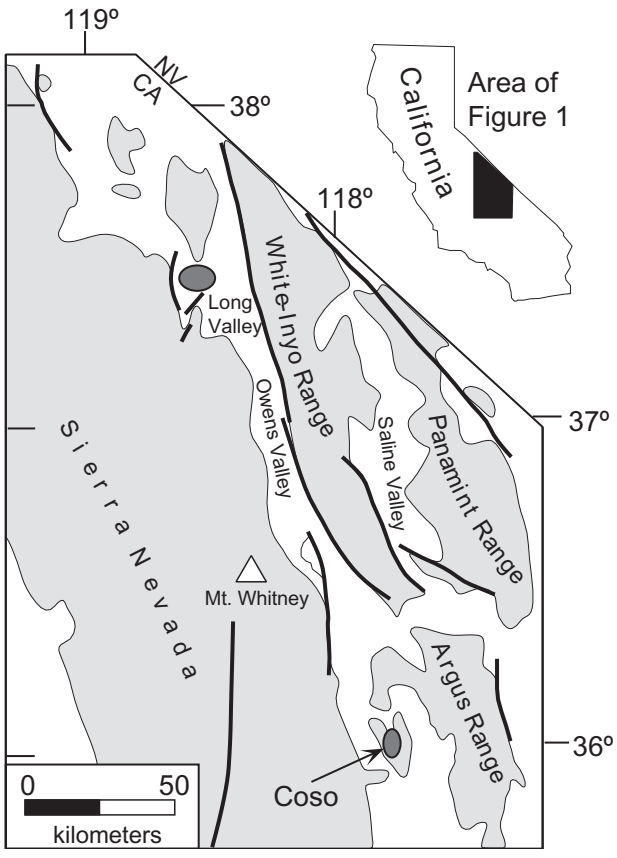

Fig. 1. Location of Coso Volcanic field at southern end of Owens Valley, CA. Ranges are shaded and major Pliocene-recent faults shown as heavy black lines. Pliocene and Pleistocene volcanic rocks sit on Mesozoic basement between Argus Range and Sierra Nevada. Modern geodetic vectors, earthquake focal mechanisms and fault displacement indicate that E–W extension and right-lateral displacement affects the Coso region.

COSO VOLCANIC FIELD AND DEVILS KITCHEN RHYOLITE

The Coso Volcanic field is located within the Coso Range, at the southern end of Owens Valley, California (Fig. 1). The volcanic field comprises approximately 35 km^3 of Pliocene ($\geq$31 km^3) and Pleistocene ($\leq$4 km^3) volcanic rocks, which cover an area of approximately 400 km^2 (Duffield *et al.*, 1980). Pliocene volcanic rocks span a compositional range from basalt to rhyolite but are dominated by intermediate rocks (Novak & Bacon, 1986), whereas the Pleistocene volcanic rocks are predominantly basalt and high-silica rhyolite. The most recent volcanic eruptions of basalt and rhyolite occurred approximately 40 kyr ago (Bacon *et al.*, 1981), and the long-term behavior of the magma system suggests that future eruptions should occur (Bacon, 1982). The Coso Range and Indian Wells Valley have been undergoing tectonic extension since the Pliocene (Duffield *et al.*, 1980), and present-day seismicity associated with extension and dextral strike-slip faulting is evident there today (Weaver & Hill, 1979; Roquemore, 1980; Monastero, 1997; Bhattacharyya & Lees, 2002; Monastero *et al.*, in preparation).

At least 39 rhyolite domes have erupted at Coso since 1 Ma; most of these eruptions have occurred since approximately 0·3 Ma (Bacon *et al.*, 1981). Two domes erupted prior to 0·3 Ma, one of which is named the Devils Kitchen dome (Fig. 2), and is the subject of the present study. The Devils Kitchen dome has a bulk sanidine K–Ar age of 587 ± 0·018 ka (Duffield *et al.*, 1980; Bacon *et al.*, 1981), and is amenable to Pb/U zircon dating by ion microprobe. One other small-volume Pleistocene dome erupted at 1 Ma, but it is not clear whether this dome is related to the rhyolite system that fed the Devils Kitchen dome or any of the other younger domes. The 1 Ma dome is near the eastern periphery of the field, and is predominantly holocrystalline rhyolite, with some minor zones of perlite, whereas all other domes consist of variably hydrated but otherwise fresh, glassy rhyolite

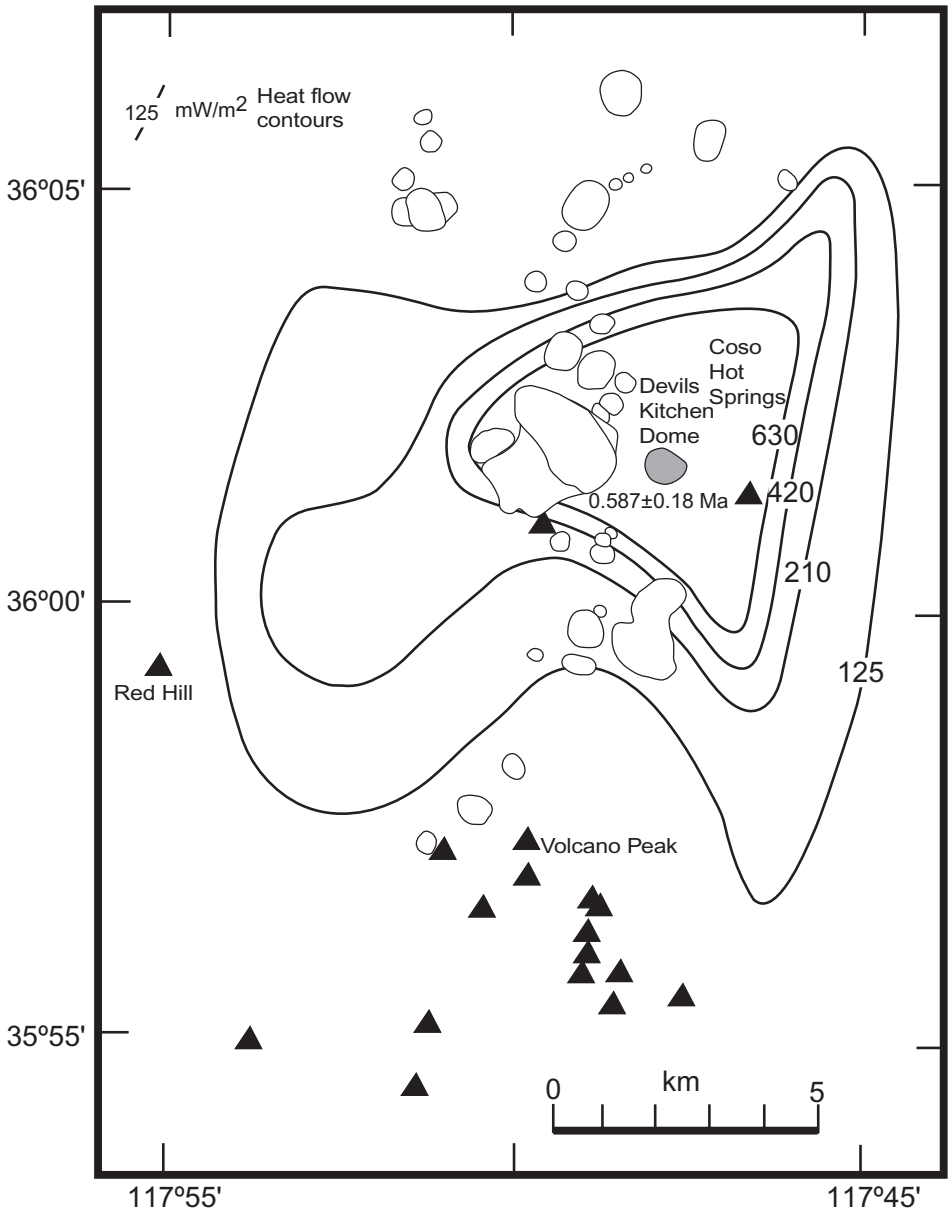

Fig. 2. Map showing outlines of Pleistocene Coso rhyolite domes and locations of Pleistocene basalt vents (▲) (from Duffield & Bacon, 1980). The Devils Kitchen dome is shown in gray with K–Ar age. Other domes are <300 ka. Note that the Devils Kitchen dome is centered near the present heat flow maximum.

obsidian and pumiceous rhyolite. The 1 Ma dome also has a Nd-isotopic composition that is markedly distinct from all the other rhyolite domes at Coso (J. Miller, unpublished data). We, therefore, do not consider this dome to be related to the main Pleistocene dome field. However, it does indicate that rhyolite magma was in the crust in the Coso area at least 400 kyr before eruption of the Devils Kitchen dome.

Because the Devils Kitchen dome is less than 500 m from the youngest dome in the field, and sits close to the center of the highest present-day near-surface heat flow (Combs, 1980; Fig. 2), we presume that the heat and mass source that ultimately gave rise to the Devils Kitchen dome has remained approximately fixed in this area for at least 600 kyr.

GEOCHEMISTRY AND PETROGRAPHY

All of the Pleistocene domes and flows are metaluminous, high-silica (≈ 77 wt %) rhyolite, with remarkably similar

major element compositions but differing somewhat in abundances of minor and trace elements (Bacon *et al.*, 1981). The trace element data combined with K–Ar ages for some of the domes allowed Bacon *et al.* (1981) to group the domes into age-related and chemically related groups, which they inferred were fed from the top of a large-volume (several hundred km^3), zoned rhyolite reservoir.

Most of the rhyolites are nearly aphyric, except the Devils Kitchen, which has 15 vol. % crystals. Minerals present in the rhyolites include quartz, sanidine, sodic oligoclase, biotite, hornblende, titanomagnetite, ilmenite, fayalite, orthopyroxene, clinopyroxene, and accessory titanite, apatite, allanite and zircon (Bacon *et al.*, 1981; Manley & Bacon, 2000). The Devils Kitchen dome specifically includes all of the major phases mentioned above plus accessory apatite and zircon. Manley & Bacon (2000) showed that orthopyroxene, clinopyroxene and some plagioclase in the Devils Kitchen rhyolite are probably xenocrysts.

The Devils Kitchen dome also contains abundant, highly porphyritic, mafic magmatic inclusions (53–56 wt % SiO_2) that are hybrids of mafic and felsic magmas, and that were incorporated into the rhyolite in a liquid state (Bacon & Metz, 1984). The inclusions have diktytaxitic textures and contain crystals of forsteritic olivine, clinopyroxene and plagioclase derived from basalt, and clinopyroxene, fayalitic olivine, quartz, sodic plagioclase, Fe–Ti oxides, hornblende, biotite, orthopyroxene and zircon derived from rhyolite. The porphyritic andesite inclusions in the Devils Kitchen rhyolite also contain centimeter-sized and smaller basalt 'droplets' (Bacon & Metz, 1984). Bacon & Metz showed that the felsic end-member that mixed with basalt to form the inclusion magma had a unique low-Ba chemical signature, which they speculated was from a zone of rhyolite beneath the magma that erupted to form the Devils Kitchen dome, but which was less fractionated than the Devils Kitchen rhyolite. Later-erupted rhyolite domes also contain quenched magmatic inclusions, but, in all these cases, the inclusions are aphyric andesites that generally have higher SiO_2 contents (55–60 wt %; Bacon & Metz, 1984).

Geobarometric estimates for the Devils Kitchen rhyolite place the magma body that fed the dome at a depth of approximately 12 km, and magmatic phenocrysts (oxides, hornblende–plagioclase, and ternary feldspars) record an equilibrium temperature of 740 ± 25°C (Manley & Bacon, 2000). Pre-eruptive water contents have not been determined for the Devils Kitchen dome; however, rhyolite, erupted to form the younger domes, was vapor-saturated with water-rich fluid (Blouke, 1993; Newman *et al.*, 1993; Manley & Bacon, 2000). Manley & Bacon (2000) argue that a free vapor phase was present in the Devils Kitchen magma body, based on bubble volumes for large vapor bubbles versus shrinkage bubbles in melt inclusions from the Devils Kitchen rhyolite, and by comparisons with melt inclusions in phenocrysts from younger domes.

ANALYTICAL METHODS AND DATA REDUCTION

Zircons from the Devils Kitchen rhyolite (generally $\geq 100\,\mu m$) were separated by standard procedures, and then mounted in epoxy resin and polished to expose zircon cores. The zircons were then imaged using a CL detector on the scanning electron microscope in the Stanford–USGS Micro-Analytical Center (SUMAC). The CL images were further enhanced for contrast and detail using Adobe Photoshop™.

After CL imaging, the mount was acid-rinsed and the zircons were photographed in transmitted light. The mount was then Au coated and placed in the sample chamber of the SHRIMP-RG (reverse geometry) at SUMAC. For each analysis, an 8 nA $^{16}O^{2}$-primary ion beam was rastered across the grain for 2 min, to remove the gold coat and surface contamination. Positive secondary ions were then collected by excavating an approximately 1 μm deep flat-floored, elliptical (approximately 25 μm × 35 μm) pit. For each analysis, six scans of peaks at $^{90}Zr_2{}^{16}O$, ^{204}Pb, ^{206}Pb, ^{207}Pb, ^{238}U, $^{232}Th^{16}O$ and $^{238}U^{16}O$ were collected. Beam tuning and centering was done using the $^{238}U^{16}O$ peak, with maximum count times for ^{206}Pb and ^{207}Pb of 14 s.

Data were referenced to the AS57 zircon standard (1099 Ma) and the SUMAC R33 internal standard, which was analyzed repeatedly during the analysis period. Uranium concentrations were obtained by comparison with zircon standard SL13. Data reduction was done using SQUID 1.02 (Ludwig, 2001), and reported ages ($^{206}Pb/^{238}U$ ages) for all analyses utilize the Pb isotopic ratios for sanidine for the Devils Kitchen dome in Bacon *et al.* (1984) for the common Pb correction.

RESULTS

Cathodoluminescence images

Cathodoluminescence images show that internal zoning textures are highly variable and commonly quite complex (Fig. 3). Brightness contrasts in the zircons are a function of U-content, with high-U zones corresponding to dark zones of crystals.

Zircons may show fine-scale oscillatory zoning (Fig. 3a), or may instead be weakly zoned (Fig. 3b). Although most zircons are euhedral, many also have anhedral, embayed cores with euhedral overgrowths (Fig. 3c). In many zircons, there are multiple, internal surfaces that clearly truncate well-developed crystal zoning (Fig. 3d). Additionally, the CL images indicate qualitatively that

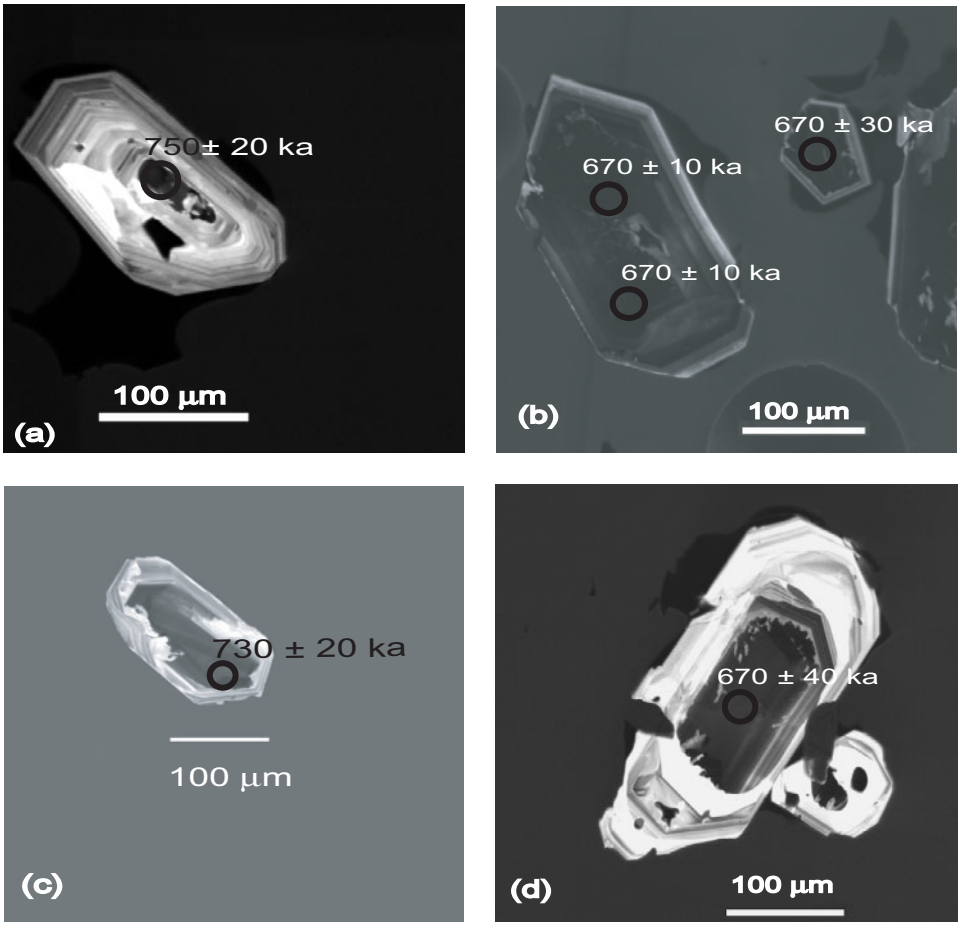

Fig. 3. (a) Euhedral oscillatory zoned zircon structure observed in some zircons. Note that this sample has an anhedral high-U core (dark) that is less than 50 μm in maximum dimension. Oscillatory zones are truncated (on the left side of grain) by a zone of U-poor (white) zircon that is, in turn, surrounded by an outer rim of fine-scale zoned zircon. (b) Euhedral, high-U, weakly zoned zircons. Zoning is slight throughout most of the grain but most also have a thin (<10 μm) rim of slightly lighter gray (in CL) that may be an edge artifact. (c) Zircon with large, weakly zoned U-rich core that is strongly resorbed and overgrown by less U-rich zircon. U-rich core indicates that high-silica rhyolite was present early in the development of the system, and that the early rhyolite zircons were recycled in later rhyolite. The outer oscillatory growth zones have also been clearly truncated by later zones. (d) Large, complexly zoned zircon, showing a minimum of four (and probably more) pronounced resorption and subsequent growth events. Individual spot ages for analyzed cores are also shown on all images. Note that the total age range spanned by the cores shown here is approximately 80 kyr. See text for further discussion.

U concentration ranges widely both within and between grains, and that grains have U-rich cores overgrown by U-poor rims and vice versa.

Both CL and transmitted light imaging showed that all of the zircons analyzed were surrounded at least partially by rhyolite glass, indicating that the zircons were in contact with rhyolite melt in the magma prior to eruption (i.e. were not occluded in other phases).

Concentration and age data

Concentrations of U and Th, $^{206}Pb/^{238}U$ ratios, and age data with errors for zircon cores and rims are given in Table 1. The requirement that the zircon should have enough radiogenic Pb for a robust analysis tends to favor analysis of U-rich zircons, although, during analysis, we attempted to analyze zircons with a wide variety of zoning characteristics. Perusal of the zircons in CL images suggests that approximately 60–70% of them are qualitatively high-U and Th zircons.

Concentrations of U and Th in some of the zircons (or zones within zircons) are exceptionally high, in comparison with zircons from other silica-rich rocks (>10 000 ppm U for the most U-rich zircons and >5000 ppm Th for the most Th-rich zircons). Within the sample population of zircons, the concentrations vary over two orders of magnitude, and concentration ranges for U and Th observed within some zircons vary by 10–20× (e.g. compare core analysis 2-15A with rim analysis 2-15B in Table 1). Examination of all the data for population subgroups

Table 1: Analytical data for the Devils Kitchen zircons

Analysis	U (ppm)	Th (ppm)	$^{206}Pb/^{238}U$	± error	$^{207}Pb/^{206}Pb$	± error	Model ages (Ma)	error (Myr)
Cores								
2-2A	2900	1320	0·00013	0·00001	0·28	0·04	0·67	0·08
2-3A	6900	4160	0·00015	0·00001	0·28	0·04	0·73	0·06
2-6A	8000	3720	0·00034	0·00004	0·57	0·02	0·80	0·06
2-8A	9200	8140	0·00009	0·00001	0·10	0·01	0·66	0·02
2-9A	5400	2200	0·00008	0·00001	0·04	0·02	0·61	0·02
2-10A	5300	3000	0·00010	0·00001	0·07	0·02	0·73	0·03
2-13A	6700	3400	0·00008	0·00001	0·06	0·02	0·61	0·03
2-14A	8900	3500	0·00008	0·00001	0·04	0·01	0·61	0·03
2-15A	1000	700	0·00010	0·00002	0·18	0·07	0·60	0·08
2-17A	3400	1800	0·00008	0·00001	0·06	0·02	0·54	0·04
2-18A	17000	11000	0·00011	0·00001	0·25	0·04	0·60	0·04
2-20A	13000	6100	0·00010	0·00001	0·13	0·01	0·67	0·03
2-21A	9500	4500	0·00008	0·00001	0·05	0·01	0·61	0·03
2-22A	14000	8900	0·00008	0·00001	0·07	0·01	0·60	0·02
2-23A	2900	7900	0·00009	0·00001	0·12	0·02	0·60	0·04
2-24A	10000	5300	0·00014	0·00003	0·35	0·04	0·61	0·06
2.1	11000	6200	0·00009	0·00001	0·06	0·01	0·67	0·01
2.2	7400	3100	0·00009	0·00001	0·11	0·02	0·67	0·03
3.1	13000	7700	0·00010	0·00001	0·10	0·01	0·67	0·01
3.2	12000	7400	0·00009	0·00001	0·07	0·01	0·67	0·01
6.1	4700	2500	0·00009	0·00001	0·06	0·01	0·67	0·04
8.1	800	500	0·00010	0·00003	0·16	0·08	0·60	0·10
9.1	2300	900	0·00022	0·00002	0·44	0·03	0·80	0·05
11.2	4000	2100	0·00010	0·00001	0·06	0·01	0·73	0·02
12.1	2800	2100	0·00014	0·00002	0·24	0·04	0·73	0·06
13.1	300	100	0·00011	0·00003	0·21	0·06	0·67	0·08
15.1	24000	15000	0·00012	0·00001	0·10	0·00	0·80	0·01
16.1	200	100	0·00010	0·00003	0·14	0·06	0·60	0·08
18.1	5200	2300	0·00011	0·00001	0·06	0·01	0·80	0·02
19.1	2400	3400	0·00010	0·00002	0·15	0·03	0·64	0·05
20.1	1400	1100	0·00009	0·00001	0·14	0·03	0·60	0·03
21.1	3700	5800	0·00024	0·00002	0·54	0·02	0·57	0·05
22.1	12000	7300	0·00010	0·00001	0·09	0·01	0·67	0·01
23.1	3300	6000	0·00011	0·00001	0·06	0·01	0·75	0·02
Rims								
2-1B	22000	17000	0·00012	0·00001	0·07	0·00	0·85	0·03
2-2B	6500	2400	0·00024	0·00002	0·47	0·03	0·74	0·07
2-5B	4900	2100	0·00010	0·00002	0·28	0·05	0·54	0·06
2-6B	5700	2000	0·00008	0·00001	0·08	0·01	0·61	0·03
2-6C	2000	500	0·00007	0·00001	0·11	0·06	0·55	0·06
2-7A	2390	1000	0·00008	0·00001	0·08	0·02	0·61	0·06
2-7B	4400	2400	0·00009	0·00001	0·10	0·02	0·60	0·05
2-8B	1500	800	0·00007	0·00001	0·08	0·03	0·54	0·04
2-9B	6200	3400	0·00008	0·00001	0·06	0·01	0·60	0·02
2-9C	2900	1160	0·00008	0·00001	0·06	0·02	0·61	0·03

Table 1: continued

Analysis	U (ppm)	Th (ppm)	$^{206}Pb/^{238}U$	± error	$^{207}Pb/^{206}Pb$	± error	Model ages (Ma)	error (Myr)
2-11A	1700	1740	0·00010	0·00001	0·33	0·05	0·52	0·05
2-12A	8800	3950	0·00008	0·00001	0·07	0·01	0·54	0·02
2-12B	7500	3200	0·00019	0·00002	0·57	0·06	0·48	0·09
2-14B	2400	800	0·00015	0·00002	0·41	0·05	0·61	0·07
2-15B	12000	6500	0·00008	0·00001	0·08	0·01	0·54	0·03
2-16B	8500	7000	0·00010	0·00001	0·05	0·01	0·72	0·04
2-17B	7900	4600	0·00008	0·00001	0·07	0·01	0·60	0·04
2-19A	9600	4900	0·00008	0·00001	0·13	0·02	0·54	0·02
2-23B	2900	900	0·00008	0·00001	0·13	0·03	0·55	0·04
1.1	6300	3000	0·00012	0·00001	0·22	0·02	0·64	0·02
1.3	900	400	0·00010	0·00002	0·13	0·03	0·58	0·04

$^{206}Pb/^{238}U$ and $^{207}Pb/^{206}Pb$ are measured ratios, with 1σ errors given. Model $^{206}Pb/^{238}U$ ages with 1σ errors reported in Table 1 are corrected for common Pb using a $^{207}Pb/^{206}Pb = 0{\cdot}811$ from sanidine from the Devils Kitchen rhyolite (Bacon *et al.*, 1984) and for initial $^{234}U-^{230}Th$ disequilibria following Schärer *et al.* (1984), using individual Th/U ratios for zircons, Th/U = 3 for the Devils Kitchen rhyolite (Bacon *et al.*, 1981), and the relation $f = (Th/U_{zircon}/Th/U_{magma})$; ^{234}U and ^{238}U are assumed to be in secular equilibrium. Data are referenced to the AS57 zircon standard (1099 Ma) and the SUMAC R33 internal standard, which was analyzed repeatedly during the analysis period. U concentrations were obtained by comparison with zircon standard SL13, assumed to have homogeneous U = 238 ppm and Th = 21 ppm. Raw data reduction was done using SQUID 1.02 (Ludwig, 2001).

based on Th/U ratio did not yield any meaningful correlation, although it is worth noting that the average Th/U ratio of cores is somewhat higher than rims (0·66 vs 0·50, respectively). It is also important to note that concentrations reported for rims in Table 1 vary considerably. Thus, whereas individual analyses generally sampled chemically homogeneous growth zones, the zircon rims, as analyzed, are not in chemical equilibrium with each other or the magma. Analysis of zircon crystal faces (e.g. Reid & Coath, 2000) might be expected to produce a much narrower spread in U and Th concentration.

Additionally, because U is strongly partitioned into zircon relative to Th, zircons will be deficient in ^{206}Pb, owing to a deficiency in ^{230}Th in the zircons relative to the magma. Calculated ages must, therefore, account for this disequilibrium (e.g. Mattinson, 1973; Schärer, 1984; Reid & Coath, 2000; Bacon *et al.*, 2000; Schmitz & Bowring, 2001; Schmitt *et al.*, 2003).

Tera–Wasserburg diagrams for core and rim analyses (Fig. 4), without common Pb correction, show the generally radiogenic character of most grains. There is no correlation between measured $^{206}Pb/^{238}U$ and U concentration, despite the large variations in U concentration and extraordinarily high U concentrations for some zircons (see inset in Fig 4a). Zircon cores and rims give age intercepts with a modified (disequilibrium-corrected) concordia (Wendt & Carl, 1985; Bacon *et al.*, 2000; Schmitt *et al.*, 2003) of 698 ± 0·024 ka (MSWD = 5·8) and 650 ± 0·066 ka (MSWD = 10·2), respectively (Fig. 4). Intercepts with modified concordia (Wendt & Carl, 1985) were calculated using an initial $(^{230}Th)/(^{238}U)$ of 0·166 and assuming an initial $(^{234}U)/(^{238}U) = 1$, where parentheses indicate activity ratio. This $(^{230}Th)/(^{238}U)$ is estimated from $f = (Th/U_{zircon}/Th/U_{magma})$ (Schärer, 1984), with the average Th/U_{zircon} taken from rim analyses in Table 1 and $Th/U_{magma} = 3$ (Bacon *et al.*, 1981). Using average Th/U for cores and rims in Table 1 and the lowest measured values of $^{232}Th/^{238}U$ in the ion probe data gives an estimated range of initial $(^{230}Th)/(^{238}U) = 0{\cdot}16$ to 0·20, in general agreement with *f*.

The age intercepts with modified concordia are significantly older than the bulk sanidine K–Ar age for the Devils Kitchen rhyolite; however, the large dispersion of the data points (indicated by high MSWD) means that the age intercepts probably have little geologic significance. The CL images clearly indicate that the zircons have had complex histories, and the highly variable Th and U concentrations suggest a growth history in strongly contrasting magmatic environments. We thus consider the distribution of zircon ages to be more meaningful.

Because the Devils Kitchen zircons have a wide range of Th/U, ranging from 0·23 to 1·8, we apply the disequilibrium correction on a point-by-point basis to all the data (e.g. Schmitt *et al.*, 2003) using the value of *f* above. After applying the disequilibrium correction, the sense of age progression is as expected for core–rim pairs, which gives us some confidence in our correction method for individual zircons (e.g. compare core analysis 2-6A with rim analyses 2-6B and 2-6C in Table 1). However, analytical errors are generally too large to realize statistically

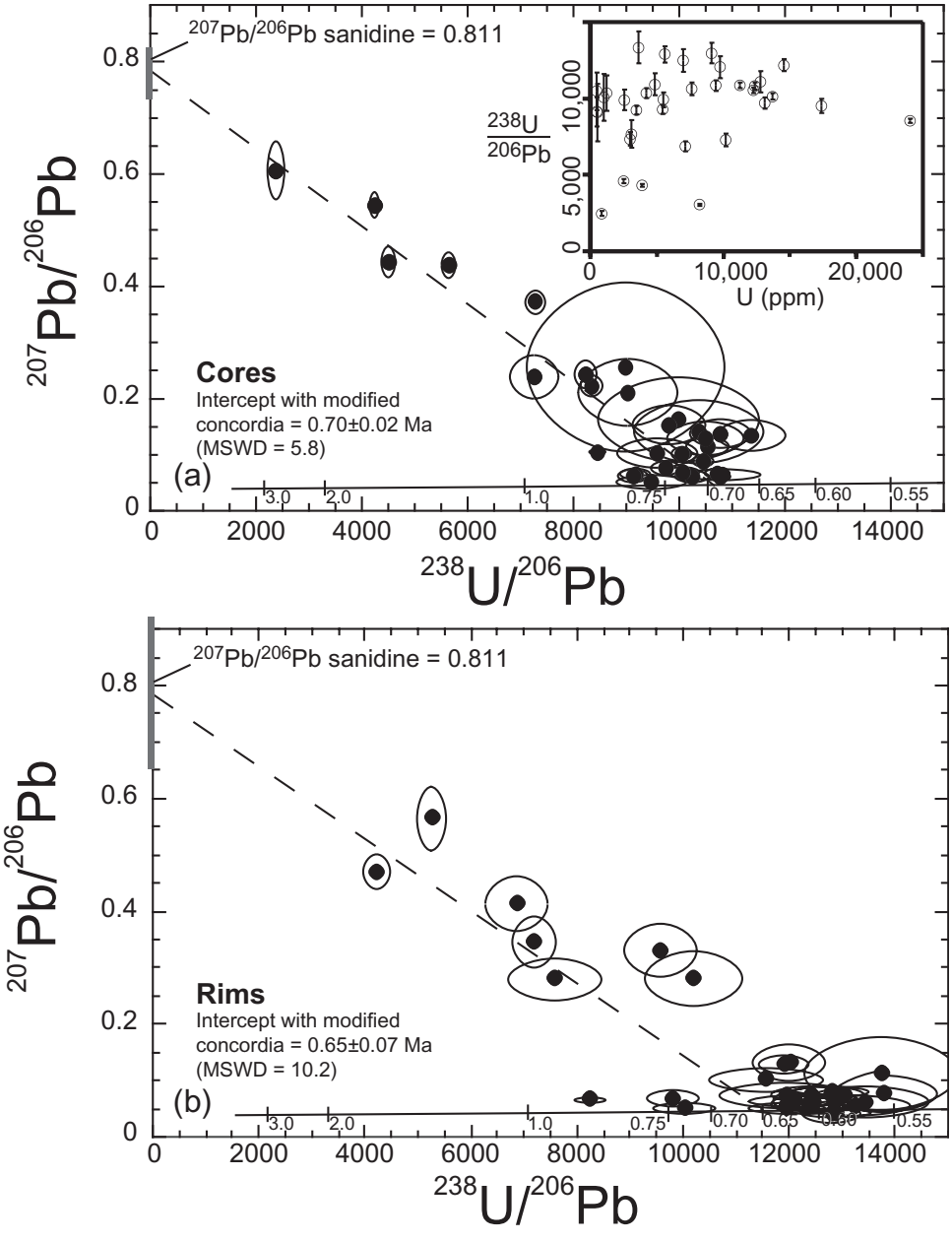

Fig. 4. Tera–Wasserburg diagram for the Devils Kitchen zircon cores (a) and rims (b). Gray box on the $^{207}Pb/^{206}Pb$ axis shows regression error of *y*-intercept and overlaps presumed common Pb ($^{207}Pb/^{206}Pb = 0{\cdot}811$) from sanidine analysis in Bacon *et al.* (1984). Individual ages and 1σ error ellipses are uncorrected for U–Th disequilibrium. Regression lines show intercepts with concordia that are modified to account for initial U–Th disequilibrium (e.g. Wendt & Carl, 1985; Bacon *et al.*, 2000; Schmitt *et al.*, 2003). Note high MSWDs of regressions, indicating appreciable scatter in the data. Inset in (a) indicates that there is no systematic correlation between U concentration and $^{206}Pb/^{238}U$ ratio (or age). See text for further discussion.

significant age differences for analyses of rim and core from any single zircon. Changing the Th/U ratio of the magma by 50% results in no appreciable difference in calculated zircon age (<1%).

Zircon core analyses (Fig. 5) span a minimum of 175 kyr, including all ages and uncertainties (Fig. 5a). A pronounced age spike is apparent on the cumulative age probability plot for core analyses at about 670 ka, and another peak is evident at about 620 ka (Fig. 5b). Ten core analyses are older than 700 ka, and these older ages produce a broad tail on the high-age side of the cumulative age probability maximum, with subordinate peaks at 730 and 800 ka (Fig. 5b). Zircon rim ages (Fig. 6) span a minimum range of 200 kyr (Fig. 6a), including all ages

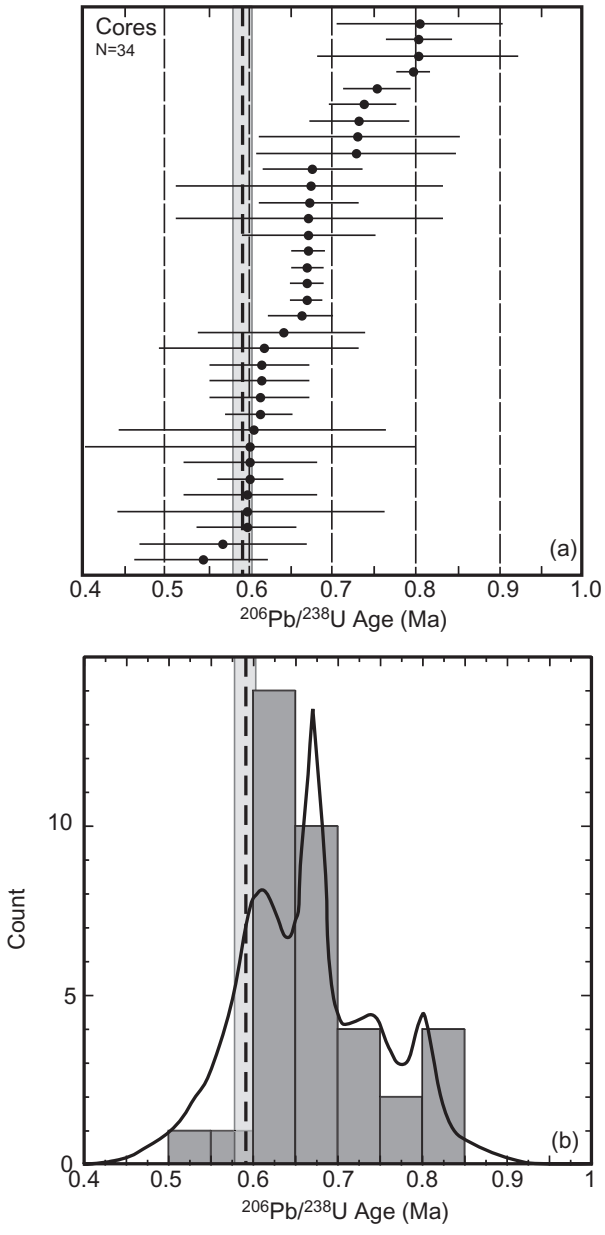

Fig. 5. $^{206}Pb/^{238}U$ ages (a) and histograms with cumulative age probability curves (b) for the Devils Kitchen zircon cores. Data are corrected for U–Th disequilibrium. Dashed line and gray box show K–Ar sanidine age for the Devils Kitchen dome and reported error (Bacon *et al.*, 1981). Ages in (a) arranged from oldest (top) to youngest (bottom). Core ages define a sharp age maximum at about 670 ka (b), which precedes the sanidine (eruption?) age by 75–80 kyr. A second peak occurs at an age of about 600 ka (b), and within the error of the sanidine age (compare with Fig. 7). Age data, including combined uncertainties for cores, indicate that zircon ages span approximately 200 kyr.

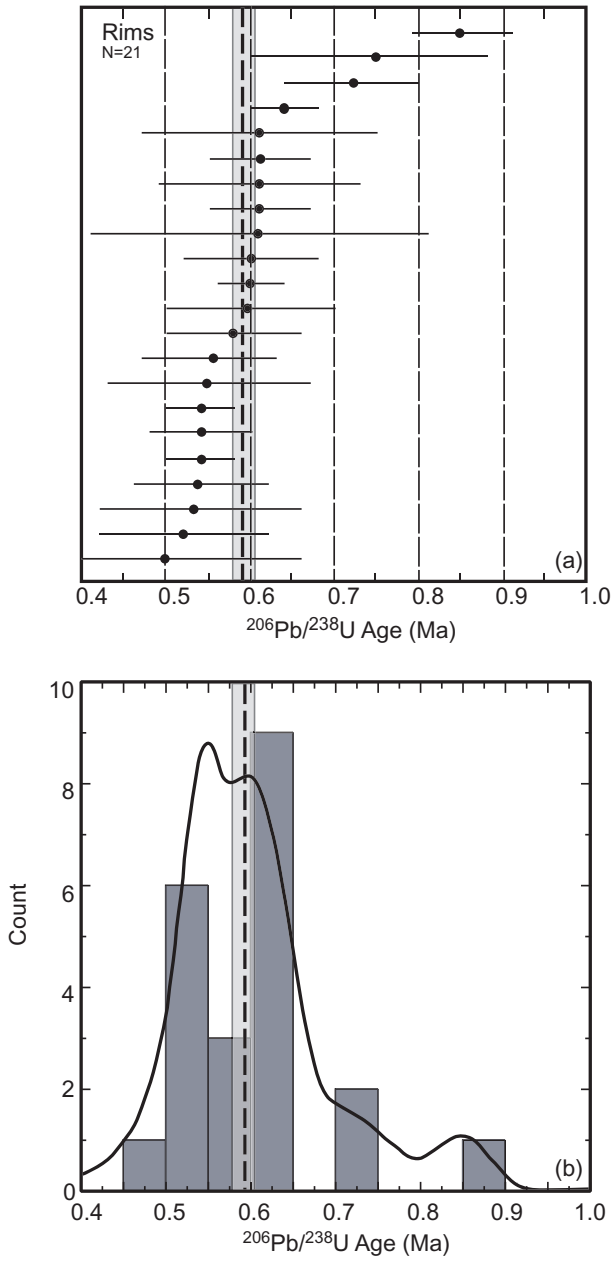

Fig. 6. $^{206}Pb/^{238}U$ ages (a) and histograms with cumulative age probability curves (b) for the Devils Kitchen zircon 'rims'. Data are corrected for U–Th disequilibrium. Dashed line and gray box show K–Ar sanidine age for the Devils Kitchen dome and reported error (Bacon *et al.*, 1981). Ages in (a) arranged in age order from oldest (top) to youngest (bottom). Rim ages define a broad 'double-humped' age maximum that straddles the reported K–Ar age. Considering the likely error in the bulk sanidine K–Ar age, it is unclear whether the youngest zircons are clearly younger than sanidines in the Devils Kitchen rhyolite. However, the youngest zircon rim ages reported here may be closer to the true 'eruption' age for the Devils Kitchen dome (approximately 550 ka?). Note also that although the majority of rim ages are younger than the 670 ka maximum observed in core ages (compare with Fig. 6), a few older rim ages are observed. These zircons could not have spent much time immersed in melt that was much younger than their observed age, and were therefore probably entrained shortly before eruption.

and uncertainties. The cumulative age probability plot for rims displays a broad 'double-humped' peak that overlaps the sanidine K–Ar age. Nine of the rims give ages that are younger than the K–Ar age. Individual age

errors for most of the nine youngest ages overlap the K–Ar age within 1σ error (Fig. 6b), but the ages and their uncertainties yield a cumulative age probability maximum at 550 ka, which is younger than bulk K–Ar age and quoted age error in Bacon *et al.* (1981). Three rim analyses give appreciably older ages (one with a large error), producing a broad tail in the high-age side of the cumulative age curve (Fig. 6b). It is also important to note that out of 55 total analyses, of which >60% were core analyses, no old 'xenocrystic' or inherited (i.e. pre-Pleistocene) zircons were found.

DISCUSSION

Initiation of the Devils Kitchen magma system and eruption age of the Devils Kitchen rhyolite

The zircon age data presented above indicate that rhyolite resided beneath the Devils Kitchen area, which was the site of the highest present-day heat flow, up to 200 kyr before any magma was erupted in this area, if we assume that the K–Ar age is the closest estimate to the eruption age. This may, therefore, correspond to the time that the Devils Kitchen magma system was initiated, i.e. approximately 800 ka. As discussed above, although one Pleistocene dome was erupted at 1 Ma at the eastern periphery of the field, it is unlikely that this dome is related to the Devils Kitchen system. Consistent with that interpretation is that no 1 Ma zircons were discovered among the Devils Kitchen zircons that we analyzed.

The published K–Ar age of 587 ± 0·018 ka (Duffield *et al.*, 1980; Bacon *et al.*, 1981) is a bulk sanidine age, and could undoubtedly be improved by single-crystal Ar–Ar dating of sanidine from the Devils Kitchen. The disequilibrium-corrected 550 ka age peak for rims reported here may be closer to the true eruption age if the bulk K–Ar age suffers from any appreciable excess Ar. As noted above, the concentrations of U and Th vary appreciably for rims, indicating they are not in equilibrium with each other or the magma. Thus, any age based on pooled ages used to define an eruption age may not be a true minimum, although rim ages should more closely approach the age at eruption. Regardless of the uncertainty in the true eruption age, the Pb/U data show that the magma system that eventually gave rise to the Devils Kitchen dome was active for at least 200 kyr prior to eruption of the Devils Kitchen dome.

Polycyclic zircon growth and crystal zoning

The observation that U and Th concentrations within the entire sample population of zircons ranges by up to 2 orders of magnitude and concentration varies 10–20× within many single zircons requires that zircon growth occurred in strongly contrasting chemical environments. The details of the zircon age distributions are thus worthy of consideration in more detail, especially given the petrographic evidence for complex growth and resorption histories of zircons in the Devils Kitchen rhyolite, and the widespread interest in the storage time of rhyolite magma in the crust.

Although the span of zircon ages is approximately 200 kyr, nearly half of all the ages (both core and rim ages) fall very close to 600 ka (compare Figs 5a and 6a) and indicate a significant growth event at this time. If the reported K–Ar age of 587 ka is taken as the time of eruption, then crystallization of these zircons did not appreciably predate the eruption. However, if rim ages that define a peak at about 550 ka are closer to the true eruption age, then the major zircon-forming event at 600 ka would have preceded eruption by as much as 50 kyr. The pronounced age maximum at 670 ka for cores (Fig. 5b) clearly indicates a significant zircon growth event that may have preceded the eruption by 70 kyr to perhaps as much as 120 kyr, depending on the true eruption age.

It is also notable that although individual age errors overlap considerably, few core or rim ages fall between about 620 and 670 ka (Table 1; Figs 5 and 6). This is seen most clearly in the core ages, where the cumulative age–frequency plot shows a peak at 670 ka and a somewhat broader and smaller peak at about 600–620 ka (Fig. 5b). A cumulative age–frequency plot for cores and rims together also produces two distinct peaks at 600 and 670 ka (not shown), and indicates that this is not simply a statistical artifact of splitting the data into cores and rims. Also, even though the errors do not allow resolution of age differences between individual cores and rims, the 670 ka age peak is not observed among the analyzed zircon rims (Fig. 6b). These features of the age data would suggest that 670 ka rhyolite zircons were bathed (and sometimes partially resorbed) in younger, zircon-saturated melt, in which new zircon growth occurred on the 670 ka zircons. Thus, the 670 ka zircons were not simply entrained from older intrusions shortly before eruption, but instead represent young zircons, related to the Devils Kitchen rhyolite system, that experienced magmatic recycling in some fashion. This can be contrasted with the three zircons with rim ages older than 700 ka, which could not have been resident in younger zircon-saturated melt for a long period of time prior to eruption. The smaller age peaks seen in zircon core data at about 730 and 800 ka (Fig. 5) would also be consistent with discrete zircon growth at these times, followed by recycling and incorporation in later melts. It is intriguing to note that the age peaks occur approximately every 60–70 kyr (especially noticeable in the core data), although we hesitate to attach any geologic significance to this observation, given the errors in the data.

The CL images confirm the inferences made from the age and concentration data, and provide further evidence that some zircons had a complex history of growth and resorption, whereas others appear to have had simple growth histories.

Many (though certainly not all) grains are weakly zoned and have uniformly high U and Th from core to rim (Fig. 3b). Because U and Th diffusion in zircon is exceedingly sluggish, even at magmatic temperatures well above those applicable to the Devils Kitchen rhyolite (e.g. Cherniak *et al.*, 1997; Lee *et al.*, 1997), we would expect pronounced U and Th growth zoning to develop, owing to depletion of U and Th in the melt at the crystal–melt interface during zircon growth. The lack of strong U or Th zoning within this group of zircons indicates that crystallization occurred in an environment that was sufficiently rich in U and Th at the zircon–melt interface, throughout the period of crystallization, that unzoned or weakly zoned crystals resulted.

In contrast to the unzoned or weakly zoned high-U and high-Th zircons, we also observe zircons with fine-scale oscillatory zoning, commonly superimposed on more pronounced U and Th growth zoning. However, few of these zircons show uninterrupted growth zoning. Anhedral, embayed zircon cores surrounded by euhedral overgrowths (e.g. Fig. 3c and d) indicate that the zircon was subjected to a period of dissolution, followed by a period of growth (see Robinson & Miller, 1999), in keeping with the observations made from the age data above. In nearly all zircons that show any evidence of resorption, multiple periods of growth and resorption are indicated, where magmatic zoning is clearly truncated by multiple internal dissolution surfaces (Fig. 3d). This is especially evident in zircons where extreme variations in U concentration are apparent and is therefore easiest to see in the CL images.

Zircon stability in a melt with the Devils Kitchen rhyolite composition (from Bacon *et al.*, 1981) is shown in Fig. 7 for a range of Zr and T at constant M [M = (2Ca + K + Na)/(Al·Si) in cation fractions = 1·39; Watson & Harrison, 1983; Watson, 1996]. For 100 ppm Zr in the Devils Kitchen rhyolite, we calculate a zircon saturation T of 751°C. Changing the Zr content, bulk composition or temperature could all result in changes in zircon solubility in the system (Harrison & Watson, 1983; Watson & Harrison, 1983; Fig. 6), and produce alternating dissolution and growth (e.g. Robinson & Miller, 1999). Measured Zr concentrations for dome groups 1–5 at Coso vary by $\leq$15 ppm, and bulk compositions for all rhyolites are nearly identical (Bacon *et al.*, 1981). Thus, a temperature change would be most likely to produce alternating growth and dissolution of zircons in the Devils Kitchen system. For zircons in the Devils Kitchen rhyolite held above the zircon saturation temperature [say, approximately 770°C, corresponding to the highest temperature estimates of Manley & Bacon (2000) for any of the Coso rhyolites], a 200 μm zircon should dissolve in 2000 years, and a 100 μm zircon should dissolve in about 250 years (Harrison & Watson, 1983). These are, however, likely to be minimum dissolution times, as they assume an instantaneous heating to 770°C, and holding the melt and zircons at that temperature. Zircon survivability also depends on the T–t path (Watson, 1996).

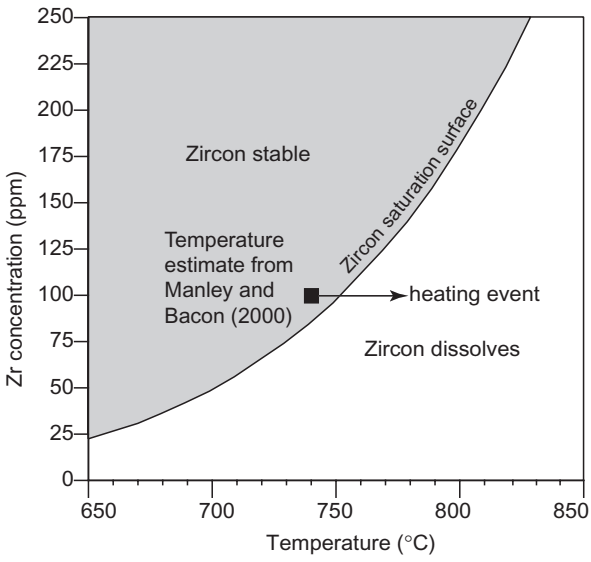

Fig. 7. Zircon stability for the Devils Kitchen zircons showing the position of zircon saturation surface as a function of Zr and T for M = 1·39 [M = (2Ca + K + Na)/(Al·Si) in cation fractions following Watson & Harrison, 1983; Watson, 1996]. Compositional data are from Bacon *et al.* (1981)]. Zircon saturation in the Devils Kitchen magma calculated at 751 ± 5°C and overlaps the temperature estimate of Manley & Bacon (2000) of 740 ± 25°C, obtained independently from two-oxide, ternary feldspar, and hornblende–plagioclase thermometry. Data suggest that at eruption, the magma temperature was just below the zircon stability limit. If ambient magma temperatures remained near that estimated by Manley & Bacon (2000), then modest heating of the rhyolite would cause zircons to dissolve. See text for further discussion.

That zircons were evidently crystallizing (as opposed to dissolving) before eruption is suggested by their uniformly euhedral character. Magma temperature was, therefore, below 750°C but probably only slightly before eruption. This is in agreement with the independent temperature determination of 740 ± 25°C for the Devils Kitchen rhyolite (Manley & Bacon, 2000) based on mineral geothermometry (Fig. 7).

A MODEL OF THE DEVILS KITCHEN MAGMA SYSTEM BASED ON OBSERVATIONS FROM ZIRCON

Any model for the rhyolite magma system that vented to form the Devils Kitchen dome must explain the complex crystallization history within the time-frame indicated

by the age data, and must be constrained by the known solubility relations of zircon. Specifically, this requires (1) growing zircons; (2) heating (dissolving) and then cooling (crystallizing) zircons; (3) transferring zircons from growth environments that were extremely U- and Th-rich to growth environments that were much poorer in U and Th, and vice versa.

A long-lived, largely liquid system?

The existence of a largely liquid and long-lived ($>10^5$ yr) body of rhyolite in the crust at Coso might be tenable, given that eruptions of rhyolite have occurred within approximately the same area for nearly 600 kyr (Duffield *et al.*, 1980; Bacon *et al.*, 1981). Furthermore, abundant Pleistocene basalt is restricted to the periphery of the rhyolite field (Bacon *et al.*, 1980), implying that a body of low-density material (rhyolite magma?) has impeded rising basalts directly beneath the rhyolite dome field since the time of eruption of the Devils Kitchen dome.

The liquid interior of a rhyolite magma body, or a highly fractionated static rhyolite cap above a chemically zoned chamber, could perhaps provide an appropriate environment for growth of unzoned or weakly zoned U- and Th-rich zircons. Growth of lower U and Th zircons, and, perhaps, oscillatory zoned zircons, might also have occurred along the cool, crystal-rich margins of the chamber. Settling of zircons from the upper part of the chamber through the interior into hotter and deeper layers would cause them to be resorbed, and they would also settle into a different chemical environment. However, settling of individual zircons of the size range analyzed from the interior is unlikely if the rhyolite is convecting (Reid *et al.*, 1997). Detachment of mushy zircon-bearing rinds from the walls within a zoned magma body might provide a way for the zircons to be carried in crystal-laden plumes into deeper and hotter parts of the chamber. In either case, however, zircons should merely dissolve. Possibly, resorbing zircons could be carried to the cooler edges or walls of the magma body by lateral convection, where they would begin to grow again.

Dissolution and regrowth could also be caused by transient heating of the resident rhyolite by basalt injections, which are an effective way of raising the temperature in rhyolite magma for short periods of time, even for a modest amount of basalt input (e.g. Sparks & Marshall, 1986). Basalt injection would induce forced convection in the rhyolite magma and would be accompanied by a temperature rise (e.g. Snyder & Tait, 1996; Couch *et al.*, 2001). Zircons would be expected to dissolve briefly following injection of basalt, and then new zircon would grow once the magma cooled back to below the temperature of zircon saturation (e.g. Fig. 7). The quenched mafic inclusions present in the Devils Kitchen rhyolite provide clear evidence of mafic magma input into the rhyolite magma body that fed the Devils Kitchen eruption (Bacon & Metz, 1984). This process can explain resorption and regrowth events, but it cannot easily explain the development of the extreme chemical zoning within, and the overall chemical variability among, the Devils Kitchen zircons.

Piecemeal assembly, solidification and remelting

Periodic freezing and thawing of small, and, perhaps, isolated, granite bodies by basaltic input (e.g. Mahood, 1990), or periodic remobilization of near-solidus crystal mush (or both), provide an alternative model to explain the polycyclic nature of the Devils Kitchen zircons, and may be more compatible with the data presented above.

The peaks in the cumulative age spectra suggest relatively discrete periods of zircon growth between periods of no growth or limited growth. New zircon growth would occur upon fresh emplacement and subsequent cooling and crystallization of rhyolite from the source, and resorption followed by crystallization would occur in response to thermal rejuvenation of mush or melting of solidified earlier granite intrusions related to development of the rhyolite system. Thus, whereas the rhyolite system could be considered active for a relatively long time (200 kyr) prior to any eruption, high melt fraction residence time(s) may have been considerably shorter (<50 kyr). The observation that fairly large (>50 μm) cores survive the heating events is also indicative of remelting or thermal events of relatively short duration (e.g. Watson, 1996).

In general, a model of multiple batches of rhyolite that solidify partially or completely and remelt is more compatible with the wide range of U and Th concentrations in the zircons, and can explain the textural evidence for pronounced resorption and transfer of zircons to strongly contrasting chemical environments. Concentrations of U and Th in growing zircons will vary markedly, depending on U and Th concentration of the initial rhyolite, and will also vary significantly depending on melt fraction, and overall melt composition during solidification. It is also not clear that growth of high-U and high-Th unzoned (or weakly zoned) zircons necessitates growth in a large-volume, largely liquid magma body.

For the most U- and Th-rich zircons (>10 000 ppm U and >5000 ppm Th), published partition coefficients (e.g. Mahood & Hildreth, 1983; Bea *et al.*, 1994; Charlier & Zellmer, 2000; Blundy & Wood, 2003) suggest that the zircons should be in equilibrium with melts having U and Th concentrations up to 10 times higher than any measured concentrations (Bacon *et al.*, 1981) for any Coso rhyolite. Such high implied melt concentrations of U and

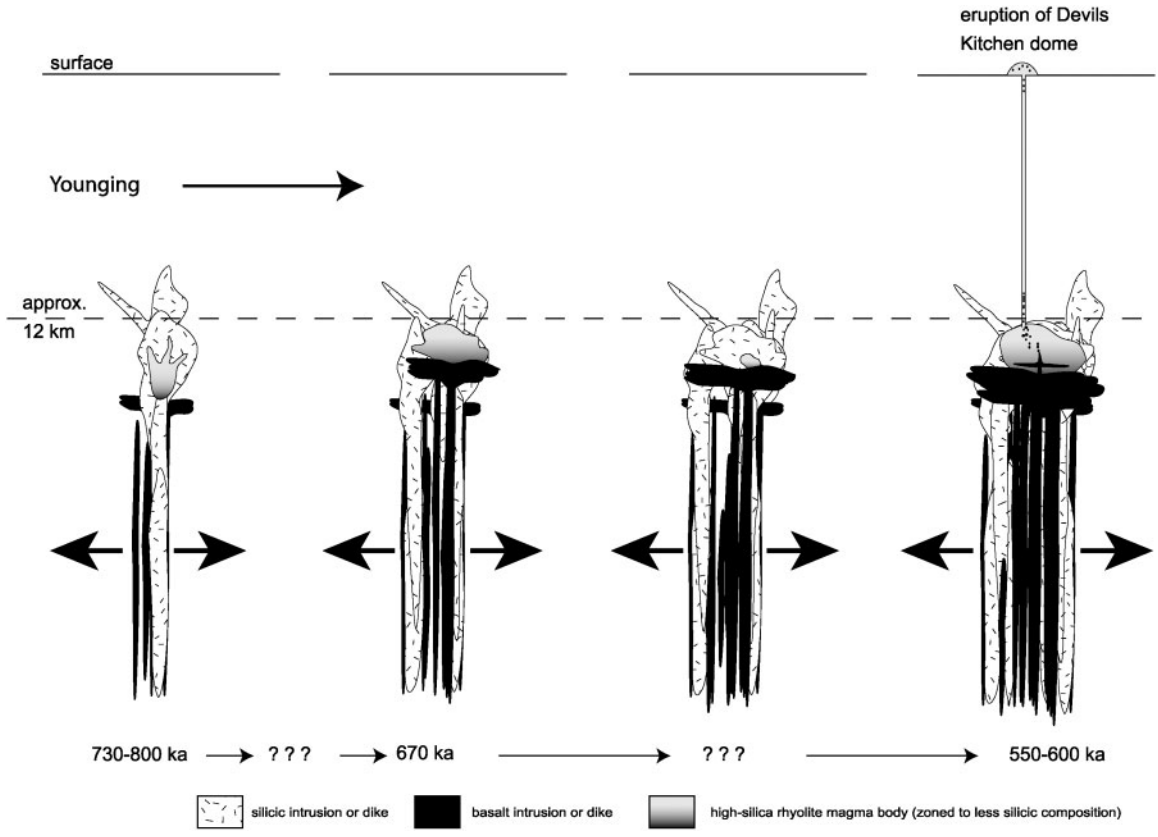

Fig. 8. Broad conceptual model of early development of rhyolite system that produced the Devils Kitchen dome eruption with age progression from left to right. The Coso area underwent tectonic extension throughout the period of development of the Devils Kitchen magma system and continues today. Initial stages of development occurred as pulses of silicic magma, probably accompanied by basaltic magma, and were emplaced between approximately 730 and 800 ka. At approximately 670 ka, significant zircon crystallization occurred, probably as a result of fresh rhyolite emplacement and/or melting of earlier solidified silicic intrusions. It is uncertain the extent to which the system solidifed between pulses, especially after 670 ka. All periods of zircon crystallization are typified by crystallization in rhyolite magma, with appreciable variations in melt fraction. Rejuvenation and direct injection of basalt in the Devils Kitchen rhyolite magma body occurred at 600 ka, forming hybrid mafic andesite inclusions (Bacon & Metz, 1984) that were entrained in Devils Kitchen rhyolite during eruption (at approximately 550 ka?). See text for further discussion of model.

Th can only be generated by extreme fractional crystallization (>95% solid), assuming perfectly incompatible behavior of U and Th, and starting with a generous amount of U (4–5 ppm) and Th (7–8 ppm) in the initial melt. Concentrations of U and Th in zircon over 0·5 wt % are rare and found primarily in highly fractionated leucogranites (i.e. pegmatites and aplites; see Speer, 1982; Miller *et al.*, 1996; Hoskin *et al.*, 2000; Belousova *et al.*, 2002). Such late-stage, near-solidus leucogranite melts may also have highly variable trace element contents. Growth of zircon in relatively low melt fraction environments (e.g. during late-stage gas filter-pressing?; Sisson & Bacon, 1999), but with a sufficient volume of melt in which to grow zircon, could perhaps explain the very high concentrations of U and Th and large variability in U and Th concentration for the zircons, with the important caveat that the quantity of zircon that can be grown at low melt fraction will probably be limited because of low Zr in the melt.

Some of the low-U and low-Th zircons may have been entrained from slightly older intermediate intrusions as rhyolite magma rose through deeper parts of the magma system. Xenocrysts of clinopyroxene, orthopyroxene and plagioclase are present in the Devils Kitchen rhyolite (Manley & Bacon, 2000), and provide evidence that it interacted with a more mafic rock or magma. However, there is clear evidence that rhyolite magma was present early in the history of the Devils Kitchen magma system, because some old cores have relatively high U and Th concentrations, and are surrounded by younger, lower-U and lower-Th rims (Fig. 3c; Table 1). Thus, at least some of the older zircons were derived from remelting very felsic rocks, rather than entrainment from deeper, more mafic rocks.

Based on the arguments outlined above, we favor a piecemeal magmatic assembly and remelting model that accompanied crustal extension to explain the complex zircon systematics in the Devils Kitchen dome (Fig. 8).

The oldest ages (730–800 ka) record the emplacement and early crystallization of pulses of silicic magma in the crust at mid-crustal depths (Manley & Bacon, 2000). The pronounced 670 and 600 ka zircon peaks mark periods of zircon growth that correspond to fresh input and crystallization of silicic magma and/or remelting of earlier solidfied silicic instrusions by emplacement of basaltic magma in the crust. We do not know to what extent the rhyolite system solidified between about 670 and 600 ka, but if our argument for near-solidus formation of some high-U and high-Th zircons is correct, then it implies that the system may have solidified completely between the two crystallization 'events'. After 600 ka, it is less clear whether significant solidification of the rhyolite system occurred but, again, zircons of this age include some very high-U and high-Th zircons. During high melt-fraction stages, zircons experienced resorption and regrowth as a result of heating by direct injection of basalt into the rhyolite chamber (e.g. Bacon & Metz, 1984). Sometime between 600 and 550 ka, Devils Kitchen rhyolite erupted, perhaps triggered by fresh basaltic input.

CONCLUSIONS

Zircons from the Devils Kitchen dome provide important new information about the earliest stages of development of the rhyolite magma system. The major conclusions of this study are summarized below.

(1) Ion microprobe Pb/U ages for zircons from the Devils Kitchen dome indicate that zircons contained in the Devils Kitchen rhyolite formed over a span of 200 kyr prior to the eruption of the rhyolite. Furthermore, some of the oldest zircons have high U and Th concentrations, which must have been produced in highly evolved rhyolite magma. Rhyolite magma was thus generated approximately 200 kyr before the Devils Kitchen dome erupted, and zircon crystallization occurred within rhyolite magma bodies that were emplaced piecemeal in the crust, 200 kyr prior to and up until eruption.

(2) Extreme variations in U and Th concentrations among zircons and within individual zones within the zircons, and CL images revealing textural evidence of multiple resorption events, indicate that the Devils Kitchen zircons crystallized in, and were transferred between, strongly contrasting magmatic environments. The extreme chemical variations are probably related to crystallization in magmatic environments with large variability in melt fraction.

(3) Age and chemical data, combined with calculated zircon saturation temperatures and resorption times, are most compatible with zircons' experiencing dissolution following heating during basaltic input into the rhyolite system. During the 200 kyr preceding the eruption, melt-poor mush or solidified silicic intrusions were periodically rejuvenated or remelted by basaltic inputs, the last of which may have only slightly preceded eruption.

ACKNOWLEDGEMENTS

Work on the Devils Kitchen dome rhyolite initiated during a post-doctoral fellowship to Miller under Navy Contract N68936-95-0389 to Allen Glazner, and funded through the Navy Geothermal Program Office at China Lake Naval Weapons Station. Additional support for this project was provided by a Junior Faculty Development Grant to J. Miller through San Jose State University. We also thank Frank Monastero and the Geothermal Program Office for generous support and encouragement of this work and for coordinating access to the Coso Volcanic field. Andy Sabin and Curtis Manley assisted in the field and Kent Ratajeski did the initial processing of the Devils Kitchen zircons. Harold Persing assisted at SUMAC. Discussions with Jake Lowenstern, Charlie Bacon, Allen Glazner, Mary Reid, Jorge Vazquez and Calvin Miller on various aspects of this study were enormously helpful. Jake Lowenstern graciously assisted with the modified concordia calculation. Jorge Vazquez, Jake Lowenstern, Olivier Bachmann and Charlie Bacon provided very helpful reviews, and we especially acknowledge the patient editorial handling of George Bergantz.

REFERENCES

Bachmann, O., Dungan, M. A. & Lipman, P. W. (2002). The Fish Canyon magma body, San Juan volcanic field, Colorado: rejuvenation and eruption of an upper-crustal batholith. *Journal of Petrology* **43**, 1469–1503.

Bacon, C. R. (1982). Time-predictable bimodal volcanism in the Coso Range, California. *Geology* **10**, 65–69.

Bacon, C. R. & Metz, J. (1984). Magmatic inclusions in rhyolites, contaminated basalts, and compositional zonation beneath the Coso Volcanic field, California. *Contributions to Mineralogy and Petrology* **85**, 346–365.

Bacon, C. R., Duffield, W. A. & Nakamura, K. (1980). Distribution of Quaternary rhyolite domes of the Coso Range, California: Implications for the extent of the geothermal anomaly. *Journal of Geophysical Research* **85**, 2425–2433.

Bacon, C. R., Macdonald, R., Smilth, R. L. & Baedecker, P. A. (1981). Pleistocene high-silica rhyolites of the Coso Volcanic field, Inyo County, California. *Journal of Geophysical Research* **86**, 10223–10241.

Bacon, C. R., Krusawa, H., Delevaux, M. H., Kistler, R. W. & Doe, B. R. (1984). Lead and strontium isotopic evidence for crustal interaction and compositional zonation in the source regions of Pleistocene basaltic and rhyolitic magmas of the Coso Volcanic field, California. *Contributions to Mineralogy and Petrology* **85**, 366–375.

Bacon, C. R., Persing, H. M., Wooden, J. L. & Ireland, T. R. (2000). Late Pleistocene granodiorite beneath Crater Lake caldera, Oregon, dated by ion microprobe. *Geology* **28**, 467–470.

Bea, F., Pereira, M. D. & Stroh, A. (1994). Mineral/leucosome trace-element partitioning in a peraluminous migmatite (a laser ablation–ICP–MS study). *Chemical Geology* **117**, 291–312.

Belousova, E. A., Griffin, W. L., O'Reilly, S. Y. & Fisher, N. I. (2002). Igneous zircon: trace element composition as an indicator of source rock type. *Contributions to Mineralogy and Petrology* **143**, 602–622.

Bhattacharyya, J. & Lees, J. M. (2002). Seismicity and seismic stress in the Coso Range, Coso Geothermal Field, and Indian Wells Valley Region, southeast-central California. In: Glazner, A. F., Walker, J. D. Bartley, J. M. (eds) *Geologic Evolution of the Mojave Desert and Southwestern Basin and Range. Geological Society of America Memoir* **195**, 243–257.

Bindeman, I. N., Valley, J. W., Wooden, J. L. & Persing, H. M. (2001). Post-caldera volcanism: *in situ* measurement of U/Pb age and oxygen isotope ratio in Pleistocene zircons from Yellowstone caldera. *Earth and Planetary Science Letters* **198**, 197–206.

Blouke, K. J. (1993). Volatile compositions of melt inclusions in Coso Range rhyolite (abstract). *Geological Society of America, Abstracts with Programs* **25**, 11.

Blundy, J. & Wood, B. (2003). Mineral–melt partitioning of uranium, thorium, and their daughters. In: Bourdon, B., Henderson, G. M., Lundstrom, C. C. & Turner, S. P. (eds) *U-Series Geochemistry. Reviews in Mineralogy & Geochemistry* **52**, 59–123.

Brown, S. J. A. & Fletcher, I. R. (1999). SHRIMP U–Pb dating of the preeruption growth history of zircons from the 340 ka Whakamaru ignimbrite, New Zealand: Evidence for >250 k.y. magma residence times. *Geology* **27**, 1035–1038.

Charlier, B. & Zellmer, G. (2000). Some remarks on U–Th mineral ages from igneous rocks with prolonged crystallization histories. *Earth and Planetary Science Letters* **183**, 457–469.

Cherniak, D. J., Hanchar, J. M. & Watson, E. B. (1997). Diffusion of tetravalent cations in zircon. *Contributions to Mineralogy and Petrology* **127**, 383–390.

Combs, J. (1980). Heat flow in the Coso geothermal area, Inyo County, California. *Journal of Geophysical Research* **85**, 2411–2424.

Couch, S., Sparks, R. S. J. & Carroll, M. R. (2001). Mineral disequilibrium in lavas explained by convective self-mixing in open magma chambers. *Nature* **411**, 1037–1039.

Duffield, W. A., Bacon, C. R. & Dalrymple, G. B. (1980). Late Cenozoic volcanism, geochronology, and structure of the Coso Range, Inyo County, California. *Journal of Geophysical Research* **85**, 2381–2404.

Harrison, T. M. & Watson, E. B. (1983). Kinetics of zircon dissolution and zirconium diffusion in granitic melts of variable water content. *Contributions to Mineralogy and Petrology* **84**, 67–72.

Hawkesworth, C. J., Blake, S., Evans, P., Hughes, R., Macdonald, R., Thomas, L. E., Turner, S. P. & Zellmer, G. (2000). Time scales of crystal fractionation in magma chambers—integrating physical, isotopic and geochemical perspectives. *Journal of Petrology* **41**, 991–1066.

Hawkesworth, C., George, R., Turner, S. & Zellmer, G. (2004). Timescales of magmatic processes. *Earth and Planetary Science Letters* **218**, 1–16.

Hoskin, P. W. O., Kinny, P. D., Wyborn, D. & Chappell, B. W. (2000). Identifying accessory mineral saturation during differentiation in granitoid magmas: an integrated approach. *Journal of Petrology* **41**, 1365–1396.

Lee, J. K. W., Williams, I. S. & Ellis, D. J. (1997). Pb, Th, and U diffusion in natural zircon. *Nature* **390**, 151–162.

Lowenstern, J. B., Persing, H. M., Wooden, J. L., Lanphere, M., Donnelly-Nolan, J. & Grove, T. L. (2000). U–Th dating of single zircons from young granitoid xenoliths: new tools for understanding volcanic processes. *Earth and Planetary Science Letters* **183**, 291–302.

Ludwig, K. R. (2001). SQUID 1.02 Add-In for Excel™. *Berkeley Geochronology Center Special Publication* **2**.

Mahood, G. (1990). Second reply to comment of R. S. J. Sparks, H. E. Huppert & C. J. N. Wilson on 'Evidence for long residence times of rhyolitic magma in the Long Valley magmatic system: the isotopic record in the precaldera lavas of Glass Mountain'. *Earth and Planetary Science Letters* **99**, 395–399.

Mahood, G. & Hildreth, W. (1983). Large partition coefficients for high-silica rhyolites. *Geochimica et Cosmochimica Acta* **47**, 11–30.

Manley, C. R. & Bacon, C. R. (2000). Rhyolite thermobarometry and the shallowing of the magma reservoir, Coso Volcanic field, California. *Journal of Petrology* **41**, 149–174.

Mattinson, J. M. (1973). Anomalous isotopic composition of lead in young zircons. *Carnegie Institution of Washington Yearbook* **72**, 613–616.

Miller, J. S., Santosh, M., Pressley, R. A., Clements, A. S. & Rogers, J. J. W. (1996). A Pan-African thermal event in southern India. *Journal of Southeast Asian Earth Sciences* **14**, 127–136.

Monastero, F. C. (1997). Evidence for a nascent metamorphic core complex at the Coso geothermal area, California. *EOS Transactions, American Geophysical Union* **78**, F659.

Newman, S., Blouke, K., Bashir, N., Ihinger, P. D. & Stolper, E. (1993). Cooling of rhyolitic volcanics: evidence from melt inclusions (abstract). *Geological Society of America, Abstracts with Programs* **25**, 43.

Novak, S. W. & Bacon, C. R. (1986). *Pliocene volcanic rocks of the Coso Range, Inyo County, California. US Geological Survey Professional Paper* **1383**, 44.

Reid, M. R. & Coath, C. D. (2000). In situ U–Pb ages of zircons from the Bishop Tuff: no evidence of long crystal residence times. *Geology* **28**, 443–446.

Reid, M. R., Coath, C. D., Harrison, T. M. & McKeegan K. D. (1997). Prolonged residence times for the youngest rhyolites associated with Long Valley Caldera: ^{230}Th–^{238}U ion microprobe dating of young zircons. *Earth and Planetary Science Letters* **150**, 27–39.

Robinson, D. M. & Miller, C. F. (1999). Record of magma chamber processes preserved in accessory mineral assemblages. *American Mineralogist* **84**, 1346–1353.

Roquemore, G. R. (1980). Structure, tectonics, and stress field of the Coso Range, Inyo County, California. *Journal of Geophysical Research* **85**, 2434–2440.

Sano, Y., Tsutsumi, Y., Terada, K. & Kaneoka, I. (2002). Ion microprobe U–Pb dating of Quaternary zircon: implication for magma cooling and residence. *Journal of Volcanology and Geothermal Research* **117**, 285–296.

Schärer, U. (1984). The effect of initial ^{230}Th disequilibrium on young U–Pb ages: the Makalu case, Himalaya. *Earth and Planetary Science Letters* **67**, 191–204.

Schmitt, A. K., Grove, M., Harrison, T. M., Lovera, O., Hulen J. & Walters, M. (2003). The Geysers–Cobb Mountain magma system, California (Part 1): U–Pb zircon ages of volcanic rocks, conditions of crystallization and magma residence times. *Geochimica et Cosmochimica Acta* **67**, 3423–3442.

Schmitz, M. D. & Bowring, S. A. (2001). U–Pb zircon and titanite systematics of the Fish Canyon Tuff: an assessment of high-precision U–Pb geochronology and its application to young volcanic rocks. *Geochimica et Cosmochimica Acta* **65**, 2571–2587.

Sisson, T. W. & Bacon, C. R. (1999). Gas-driven filter pressing in magmas. *Geology* **27**, 613–616.

Snyder, D. & Tait, S. (1996). Magma mixing by convective entrainment. *Nature* **379**, 529–531.

Sparks, R. S. J. & Marshall, L. A. (1986). Thermal and mechanical constraints on mixing between mafic and silicic magmas. *Journal of Volcanology and Geothermal Research* **29**, 99–129.

Speer, J. A. (1982). Zircon. In: Ribbe, P. H. (ed) *Orthosilicates. Mineralogical Society of America, Reviews in Mineralogy* **5**, 67–112.

Spera, F. J. & Bohrson, W. A. (2001). Energy-constrained open-system magmatic processes I: General model and energy-constrained assimilation and fractional crystallization (EC-AFC) formulation. *Journal of Petrology* **42**, 999–1018.

Vazquez, J. A. & Reid, M. R. (2002). Time scales of magma storage and differentiation of voluminous high-silica rhyolites at Yellowstone caldera, Wyoming. *Contributions to Mineralogy and Petrology* **144**, 274–285.

Watson, E. B. (1996). Dissolution, growth and survival of zircons during crustal fusion: kinetic principles, geological models and implications of isotopic inheritance. *Transactions of the Royal Society of Edinburgh: Earth Sciences* **87**, 43–56.

Watson, E. B. & Harrison, T. M. (1983). Zircon saturation revisited: temperature and composition effects in a variety of crustal magma types. *Earth and Planetary Science Letters* **64**, 295–304.

Weaver, C. S. & Hill, D. P. (1979). Earthquake swarms and local crustal spreading along major strike-slip faults in California. *Pure and Applied Geophysics* **117**, 51–64.

Wendt, I. & Carl, C. (1985). U/Pb dating of discordant 0·1 Ma secondary U minerals. *Earth and Planetary Science Letters* **73**, 278–284.